

DESIGN AND DEVELOPMENT OF A 4-DOF SCARA ROBOT FOR EDUCATIONAL PURPOSES

KHAIRUL SALLEH MOHAMED SAHARI^{1*}, KHOR HONG WENG²,
YAP WEE HAN³, ADZLY ANUAR⁴, MOHD ZAFRI BAHARUDDIN⁵
& SYED SULAIMAN KAJA MOHIDEEN⁶

Abstract. Robotics have become a common course in a lot of higher institutions. Although there are many robots available in the market, most of them are for industrial purposes and are costly. There is a need to develop low cost robots for students in higher institutions to learn the elements of robotics such as design, kinematics, dynamics, sensing and control. The aim of this project is to design and develop a mechanical structure of a SCARA robot that can perform certain tasks for educational, research and exhibition purposes such as pick and place operation. The paper discusses the steps used in design and development of a 4 degree of freedom (DOF) SCARA robot which includes specification definition, conceptual design, product development, and testing. In specification definition phase, the specifications of the SCARA robot are first determined. After that, the best conceptual design of the SCARA robot is chosen after making concept evaluation in the conceptual design phase. Then, in third phase which is the product generation, the chosen design of the SCARA robot is fine-tuned. Stress analysis using finite element analysis is carried out before a prototype is developed. The direct and inverse kinematics, dynamics of the robot are then modeled. Off shelf parts are also selected based on the derived parameters from calculations. Electronic parts such as sensors and dedicated controller using low cost microcontroller are then developed. Finally, the developed SCARA robot is tested to see whether it fits the targeted specifications.

Keywords: SCARA robot; RRPR; kinematics and dynamics; educational robotics; microcontroller

Abstrak. Robotik telah menjadi satu subjek yang biasa ditawarkan dalam kebanyakan institusi pengajian tinggi di negara ini. Walaupun terdapat banyak robot-robot yang boleh dibeli di pasaran, kebanyakannya adalah untuk kegunaan perindustrian dan berkos tinggi. Terdapat keperluan untuk menghasilkan robot berkos rendah untuk kegunaan mahasiswa dan mahasiswi di institusi pengajian tinggi negara dalam mempelajari elemen-elemen robotik seperti reka bentuk,

¹⁻⁴ Department of Mechanical Engineering, Universiti Tenaga Nasional, Jalan IKRAM-UNITEN, 43000 Kajang, Selangor, Malaysia

⁵⁻⁶ Department of Electronics and Communication Engineering, Universiti Tenaga Nasional, Jalan IKRAM-UNITEN, 43000 Kajang, Selangor, Malaysia

* Corresponding author: khairuls@uniten.edu.my

kinematik, dinamik, penderiaan dan kawalan. Kertas kerja ini membentangkan proses merekacipta dan membangunkan satu robot SCARA dengan 4 darjah kebebasan berkos rendah yang boleh digunakan untuk tujuan pembelajaran, penyelidikan dan juga pameran. Kertas kerja ini membincangkan kaedah yang digunakan dalam reka bentuk dan pembangunan robot SCARA termasuk definisi spesifikasi, reka bentuk konseptual, pembangunan produk, dan uji kaji. Dalam fasa definisi spesifikasi, parameter robot SCARA akan ditetapkan terlebih dahulu. Selepas itu, reka bentuk konseptual terbaik akan dipilih selepas membuat penilaian terhadap semua konsep-konsep dalam fasa reka bentuk konseptual. Kemudian, dalam fasa penghasilan produk, reka bentuk yang terpilih akan disempurnakan lagi. Kemudian, analisis tegasan menggunakan analisis unsur terhingga akan dijalankan sebelum prototaip dihasilkan. Kinematik langsung dan songsang, dinamik robot kemudiannya dikaji. Komponen-komponen akan dipilih berdasarkan parameter-parameter hasil analisa dan pengiraan. Komponen elektronik seperti pengesan dan pengawal menggunakan pengawal mikro kos rendah kemudiannya dipasang. Akhirnya, robot SCARA yang dihasilkan akan diuji untuk melihat sama ada ia menepati sasaran parameter-parameter yang telah ditetapkan.

Kata kunci: Robot SCARA; RRRP; kinematik dan dinamik; robot pembelajaran; pengawal mikro

1.0 INTRODUCTION

In manufacturing, assembly process plays a vital role. Introduction of fast computers and sophisticated robots, assembly automation has been growing fast in the past 20 years. Development of SCARA robots, an open-loop type manipulator that is used for assembly in production industries has been successful in speeding up assembly process. SCARA robots are used by a wide range of manufacturers, from automobiles to small electronic items. It can be programmed to handle very precise work routine and works best when handling small parts. The joints of a SCARA robot can be waterproofed in order for it to work in an underwater construction. A SCARA's ability to be remotely controlled also makes it a choice in work sites hazardous to humans, such as working with chemicals, or in environments with extreme conditions, such as in steel mill.

SCARA robot stands for Selective Compliance Assembly Robot Arm and is a horizontal-jointed articulating type robot which can rotate in x-y axis and move vertically in z-axis. Due to its structure, SCARA robot excels in pick and place operation. It provides a circular work envelope and is best suited for planar tasks. This broad movement range allows for added flexibility. A SCARA robot has high compliance in the x-y plane in the sense that the arm moves freely to accomplish the assembly task accurately. SCARA robot was first developed under the guidance of Professor Hiroshi Makino from University of Yamanashi in 1979[1]. Since then SCARA robots have been widely used in industries especially for pick and place operations. A variety of SCARA robots are available in the market as well as developed by researchers [2]-[9]. For example, Bhatia *et al.* developed an expert system-based design of SCARA robot [2]. Manjunath *et al.* developed a

Jacobian model for a 4 axis indigenously developed SCARA robot [3]. Omari *et al.* meanwhile focused on development of a high precision mounting SCARA robot system with fine motion mechanism [4]. Some researchers concentrate on improving the control of SCARA robots. Ali *et al.* for instance investigated on the H^2 control of a SCARA robot using polytopic linear parameter varying approach [5].

Although there are many SCARA robots developed, most of them are for industrial purposes and are costly. There is a need to use SCARA robots for students in higher institutions to learn elements of robotics such as design, kinematics, dynamics, sensing and control. The introduction of different types of robots in robotic courses will definitely help students to understand robotics better. They can implement what they have learned theoretically and also appreciate robotics better. This paper discusses the design and development of a low-cost and safer to use SCARA robot that can perform certain tasks for educational, research and exhibition purposes. The development of the robot also includes the development of a graphical user interface able to perform simulations and also control the developed SCARA robot. The flow of the design and development of the proposed SCARA robot is shown in Figure 1.

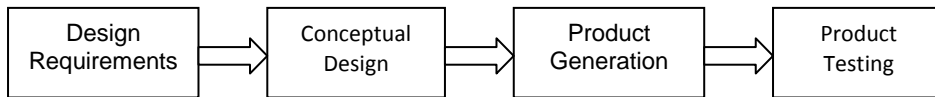


Figure 1 Design and development flow of SCARA robot

2.0 DESIGN SPECIFICATION & CONCEPTUAL DESIGN

The SCARA robot developed should have the following specification shown in Table 1. Based on the design specification, 4 conceptual designs have been developed and evaluated. Based on the application and workspace requirements, an R-R-P-R (Revolute, Revolute, Prismatic, Revolute) 4 DOF SCARA robot is chosen for the concept. Concept 1 uses belt system to revolute the second link where the motor is positioned close to the base. Concept 2 uses belt system to revolute both links. Concept 3 uses gears to revolute links 1 and 2. Concept 4 is similar to concept 2 but the motors are placed on the center of link 1. Table 2 shows the evaluation process using Decision-Matrix. Conceptual design 3 has been selected as the best alternative. Detailed design and analysis are discussed in the following chapters.

Table 1 SCARA robot design specification

Specification	Requirement
Degree of Freedom	4
Maximum payload	1 kg
Reapitability and accuracy ^s	±0.1mm
Maximum total weight ^t	15 kg

Table 2 Decision-Matrix for conceptual designs 1-4

No	Criteria	Importance	Alternatives			
			C1	C2	C3	C4
1	Movement Obstacle	20	-	-	D	S
2	Speed	25	+	-	A	-
3	Accuracy/Repeatability	30	-	S	T	S
4	Weight	15	S	-	U	-
5	Easy to manufacture	10	S	-	M	S
		Total +	1	0		0
		Total -	2	4		2
		Overall	-1	-4		-2
		Weighted Total	-25	-70		-40

3.0 FINALIZED DESIGN & KINEMATIC SYSTHESIS

Figure 2 shows the finalized design drawn using Pro- Engineering (Pro/E) software. The SCARA robot has 2 links and 4 actuators, in which 2 will be used to move the links and the other 2 to control the height and the orientation of the end effector (Figure 3). The next step will be to determine the parameters of the robot and to select the right components and parts for the robot.

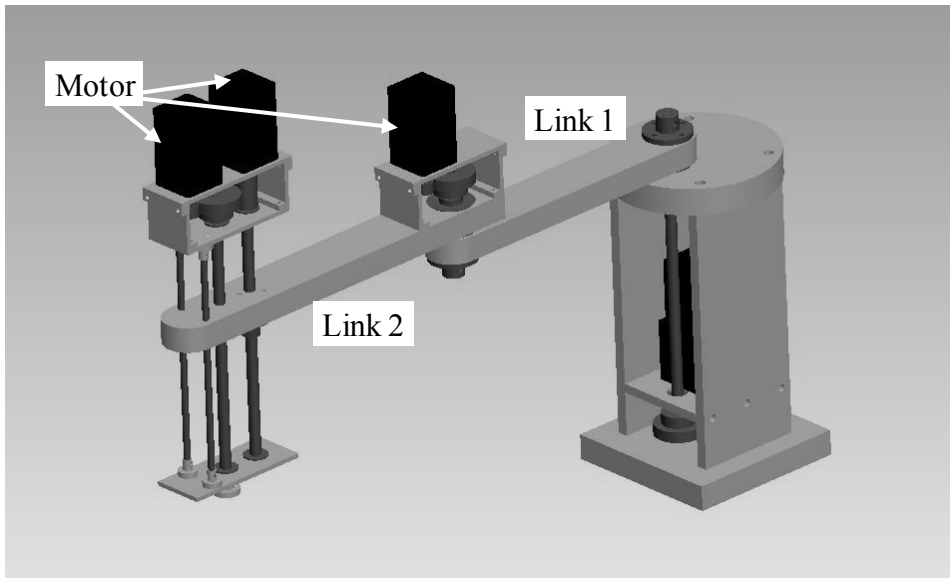


Figure 2 Finalized design of SCARA robot

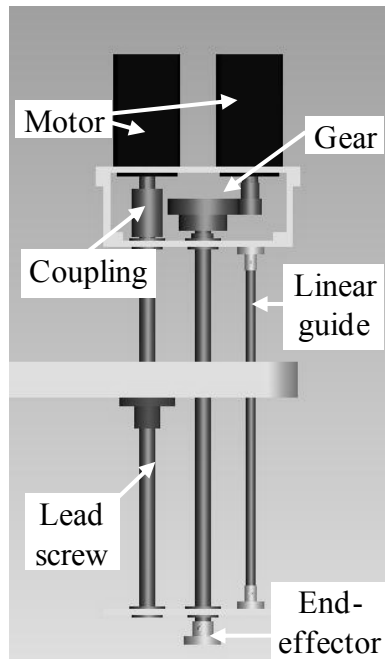


Figure 3 End effector part of the SCARA robot

Geometric structures of the SCARA robot were determined by using Denavit-Hartenberg's method. The included parameters were joint angle, link offset, link length and twist angle which represented by θ , d , a and α respectively. According to the results, the schematic diagram of the SCARA robot is described in Table 3 and Figure 4 with the dimensions.

Table 2 Denavit-Hartenberg parameters of the SCARA robot

#	θ	d	a	α
1	θ_1	302.5	250	0
2	θ_2	25	270	π
3	0	-223.5	0	0
4	θ_4	0	0	0

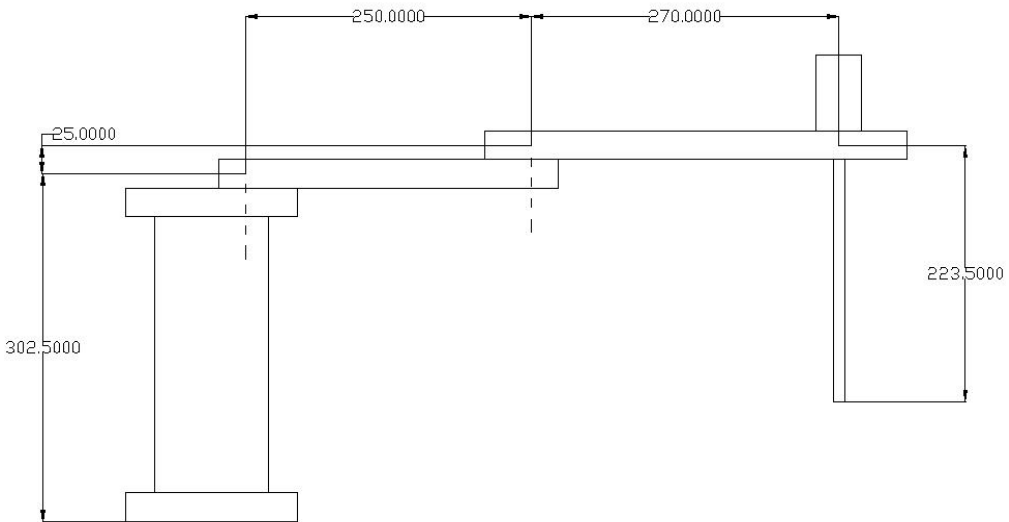


Figure 4 SCARA robot's schematic diagram

After the Denavit-Hartenberg parameters were established, the Denavit-Hartenberg transformation matrices for each joint can be obtained to solve direct and inverse kinematics as shown below.

$${}^0T_1 = \begin{bmatrix} c\theta_1 & -s\theta_1 & 0 & a_1c\theta_1 \\ s\theta_1 & c\theta_1 & 0 & a_1s\theta_1 \\ 0 & 0 & 1 & d_1 \\ 0 & 0 & 0 & 1 \end{bmatrix} \quad (1)$$

$${}^1T_2 = \begin{bmatrix} c\theta_2 & s\theta_2 & 0 & a_2c\theta_2 \\ s\theta_2 & -c\theta_2 & 0 & a_2s\theta_2 \\ 0 & 0 & -1 & d_2 \\ 0 & 0 & 0 & 1 \end{bmatrix} \quad (2)$$

$${}^2T_3 = \begin{bmatrix} 1 & 0 & 0 & 0 \\ 0 & 1 & 0 & 0 \\ 0 & 0 & 1 & -d_3 \\ 0 & 0 & 0 & 1 \end{bmatrix} \quad (3)$$

$${}^3T_4 = \begin{bmatrix} c\theta_4 & -s\theta_4 & 0 & 0 \\ s\theta_4 & c\theta_4 & 0 & 0 \\ 0 & 0 & 1 & 0 \\ 0 & 0 & 0 & 1 \end{bmatrix} \quad (4)$$

Combining all transformation matrices for each joint, the overall transformation matrix for the **SCARA** robot becomes:

$${}^0T_3 = \begin{bmatrix} c\theta_1c\theta_2 - s\theta_1s\theta_2 & -c\theta_1s\theta_2 - s\theta_1c\theta_2 & 0 & a_2(c\theta_1c\theta_2 - s\theta_1s\theta_2) + a_1c\theta_1 \\ s\theta_1c\theta_2 + c\theta_1s\theta_2 & -s\theta_1s\theta_2 + c\theta_1c\theta_2 & 0 & a_2(s\theta_1c\theta_2 + c\theta_1s\theta_2) + a_1s\theta_1 \\ 0 & 0 & 1 & -d_3 + d_1 + d_2 \\ 0 & 0 & 0 & 1 \end{bmatrix} \quad (5)$$

Based on the transformation matrix, the kinematics analysis of the **SCARA** robot can be conducted.

4.0 KINEMATICS ANALYSIS

4.1 Forward Kinematics

Forward kinematics analysis of the SCARA robot was performed in order to find the mapping between the joint displacements and the end effector's position with respect to the base frame. Kinematic parameters were determined according to Denavit-Hartenberg conventions as shown in equation (6).

$$\begin{bmatrix} P_x \\ P_y \\ P_z \\ 1 \end{bmatrix} = \begin{bmatrix} a_1 c\theta_1 + a_2 c\theta_{12} \\ a_1 s\theta_1 + a_2 s\theta_{12} \\ -d_3 + d_1 + d_2 \\ 1 \end{bmatrix} \quad (6)$$

where \mathbf{P} is the position vector of the robot hand or end effector (excluding the length of end effector).

4.2 Inverse Kinematics

While direct kinematics establishes relationship between the joint space and Cartesian space, inverse kinematics determine all possible sets of joint variables which will eventually bring the end effector to the set of desired position and orientations [10]. Based on Figure 5, the inverse kinematic equations of the SCARA robot are derived as follows:

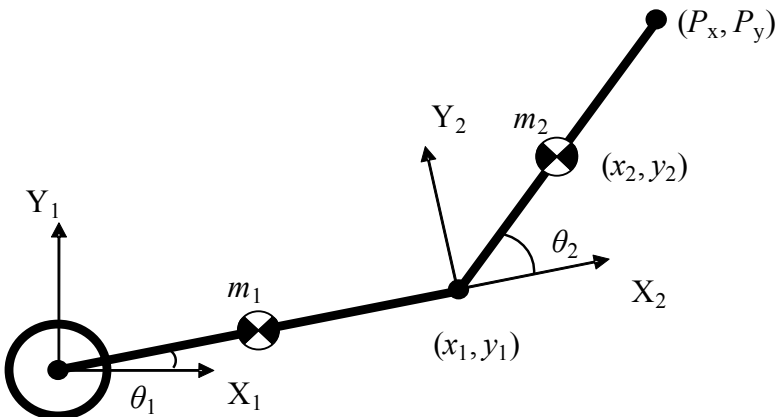


Figure 5 SCARA robot's Link 1 and Link 2

$$P_x = a_1 c \theta_1 + a_2 c \theta_{12} \quad (7)$$

$$P_y = a_1 s \theta_1 + a_2 s \theta_{12} \quad (8)$$

$$P_z = -d_3 + d_1 \quad (9)$$

$$\begin{aligned} P_x^2 + P_y^2 &= a_1^2 c^2 \theta_1 + a_2^2 c^2 \theta_{12} + 2a_1 a_2 c \theta_1 c \theta_{12} + a_1^2 s^2 \theta_1 + a_2^2 s^2 \theta_{12} + 2a_1 a_2 s \theta_1 s \theta_{12} \\ &= a_1^2 (c^2 \theta_1 + s^2 \theta_1) + a_2^2 (c^2 \theta_{12} + s^2 \theta_{12}) + 2a_1 a_2 (c \theta_1 c \theta_{12} + s \theta_1 s \theta_{12}) \\ &= a_1^2 + a_2^2 + 2a_1 a_2 c \theta_2 \end{aligned} \quad (10)$$

Rearranging Equation (10),

$$\theta_2 = \cos^{-1} \left(\frac{P_x^2 + P_y^2 - a_1^2 - a_2^2}{2a_1 a_2} \right) \quad (11)$$

Expanding Equation (7),

$$\begin{aligned} P_x &= a_1 c \theta_1 + a_2 (c \theta_1 c \theta_2 - s \theta_1 s \theta_2) \\ &= a_1 c \theta_1 + a_2 c \theta_1 c \theta_2 - a_2 s \theta_1 s \theta_2 \\ &= c \theta_1 (a_1 + a_2 c \theta_2) - s \theta_1 (a_2 s \theta_2) \end{aligned} \quad (12)$$

Expanding Equation (8),

$$\begin{aligned} P_y &= a_1 s \theta_1 + a_2 (s \theta_1 c \theta_2 + c \theta_1 s \theta_2) \\ &= a_1 s \theta_1 + a_2 s \theta_1 c \theta_2 + a_2 c \theta_1 s \theta_2 \\ &= s \theta_1 (a_1 + a_2 c \theta_2) + c \theta_1 (a_2 s \theta_2) \end{aligned} \quad (13)$$

Rearranging Equation (13),

$$s \theta_1 = \frac{P_y - c \theta_1 (a_2 s \theta_2)}{(a_1 + a_2 c \theta_2)} \quad (14)$$

Substitute Equation (14) into Equation (12) and rearranging Equation (12),

$$\begin{aligned} c \theta_1 (a_1 + a_2 c \theta_2) &= P_x + (a_2 s \theta_2) \left(\frac{P_y - c \theta_1 (a_2 s \theta_2)}{(a_1 + a_2 c \theta_2)} \right) \\ c \theta_1 (a_1 + a_2 c \theta_2)^2 &= P_x (a_1 + a_2 c \theta_2) + P_y (a_2 s \theta_2) - c \theta_1 (a_2 s \theta_2)^2 \end{aligned}$$

$$\begin{aligned}
c\theta_1 \left[(a_1 + a_2 c\theta_2)^2 + (a_2 s\theta_2)^2 \right] &= P_x (a_1 + a_2 c\theta_2) + P_y (a_2 s\theta_2) \\
c\theta_1 &= \frac{P_x (a_1 + a_2 c\theta_2) + P_y (a_2 s\theta_2)}{(a_1 + a_2 c\theta_2)^2 + (a_2 s\theta_2)^2} \\
&= \frac{P_x (a_1 + a_2 c\theta_2) + P_y (a_2 s\theta_2)}{a_1^2 + a_2^2 + 2a_1 a_2 c\theta_2}
\end{aligned} \tag{15}$$

Substitute Equation (15) into Equation (14) and rearranging Equation (14),

$$s\theta_1 (a_1 + a_2 c\theta_2) = P_y - (a_2 s\theta_2) \left(\frac{P_x (a_1 + a_2 c\theta_2) + P_y (a_2 s\theta_2)}{a_1^2 + a_2^2 + 2a_1 a_2 c\theta_2} \right) \tag{16}$$

$$\text{Let } \Delta = a_1^2 + a_2^2 + 2a_1 a_2 c\theta_2$$

$$\begin{aligned}
s\theta_1 \Delta (a_1 + a_2 c\theta_2) &= P_y \Delta - P_x (a_2 s\theta_2) (a_1 + a_2 c\theta_2) - P_y (a_2 s\theta_2)^2 \\
&= P_y (\Delta - (a_2 s\theta_2)^2) - P_x (a_2 s\theta_2) (a_1 + a_2 c\theta_2) \\
&= P_y (a_1 + a_2 c\theta_2)^2 - P_x (a_2 s\theta_2) (a_1 + a_2 c\theta_2)
\end{aligned}$$

(17)

$$\begin{aligned}
s\theta_1 \Delta &= \frac{P_y (a_1 + a_2 c\theta_2)^2 - P_x (a_2 s\theta_2) (a_1 + a_2 c\theta_2)}{(a_1 + a_2 c\theta_2)} \\
&= P_y (a_1 + a_2 c\theta_2) - P_x (a_2 s\theta_2)
\end{aligned} \tag{18}$$

$$s\theta_1 = \frac{P_y (a_1 + a_2 c\theta_2) - P_x (a_2 s\theta_2)}{\Delta} \tag{19}$$

$$\begin{aligned}
\theta_1 &= ATAN2(s\theta_1, c\theta_1) \\
&= ATAN2 \left(\frac{(a_1 + a_2 c\theta_2) P_y - (a_2 s\theta_2) P_x}{a_1^2 + a_2^2 + 2a_1 a_2 c\theta_2}, \frac{(a_1 + a_2 c\theta_2) P_x + (a_2 s\theta_2) P_y}{a_1^2 + a_2^2 + 2a_1 a_2 c\theta_2} \right)
\end{aligned} \tag{20}$$

5.0 MATERIALS

5.1 Materials Selection

Material selected to be used for the fabrication of the base and linkages is aluminum 6061. As for components that will deal with different stresses such as the arm's shaft, stainless steel will be used as stainless steel has higher ultimate strength compare to aluminum 6061. Aluminum 6061 and stainless steel were chosen because they are easy to machine and their surfaces are covered with a thin layer of oxide that helps protect the material from corrosion.

5.2 Stress Analysis

Stress analysis was carried out to determine the thickness of the links that will falls in the range of safety factor 3 to 5 after knowing the length of the links and type of material used. A safety factor of 3~5 can be considered as a suitable safety factor for this project because design with large safety factor ($N=14$) will results in the waste of materials and design with small safety factor ($N=1.5$) is not safe due to uncertainties in the data. The links were analyzed in terms of force and displacement by using Pro/Mechanica (Pro/M). Parts in which the thicknesses need to be determined are Link1 and Link2.

Assuming that a vertical 8kg load is applied on the edge of the Link1 which is made from aluminum 6061 with 23mm thickness, results of the analyses are shown in figures 6 & 7.

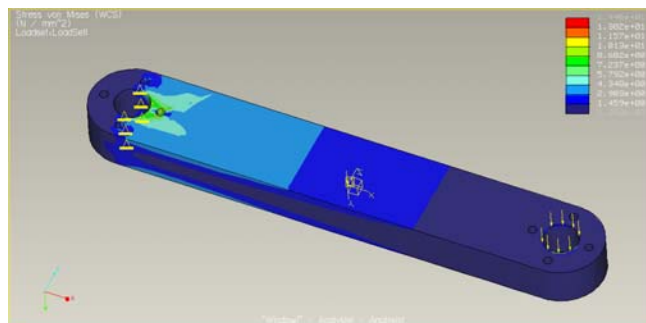


Figure 6 Stress analysis for Link1

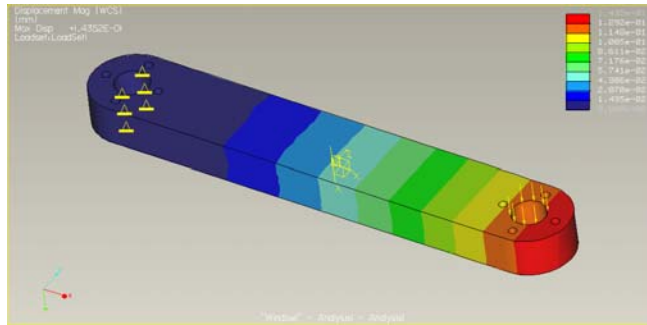


Figure 7 Displacement analysis for Link1

From Figure 6, the maximum stress σ' occurred on Link 1 is $14.46 \times 10^6 \text{ N/m}^2$. The tensile yield strength of Aluminum 6061, S_y is 55 MPa. From this, the safety factor of the link 1 is calculated to be 3.8. Since the safety factor is in the range of $3 \sim 5$, the thickness for Link1 can be considered as safe when there is an 80 N load applied on it.

From Figure 7, the maximum displacement (red colour) occurred on the edge of Link 1 is only 0.1435 mm and therefore, it would not affect much to the structure of the Link 1. The reason for this condition to occur is because several heavy components such as the motors, gripper and payload will be connected to the edge of Link 1.

From these analyses, it is safe to use aluminum 6061 with the thickness of 23mm to fabricate Link1.

Similarly, the same analyses were conducted for Link 2. Assuming a vertical 6 kg load is applied on the edge of the Link2 which is made from aluminum 6061 with 23 mm thickness, Figures 8 & 9 show the results of the analyses.

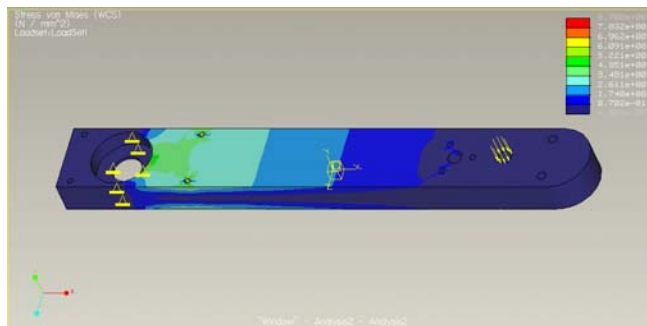


Figure 8 Stress analysis for Link2

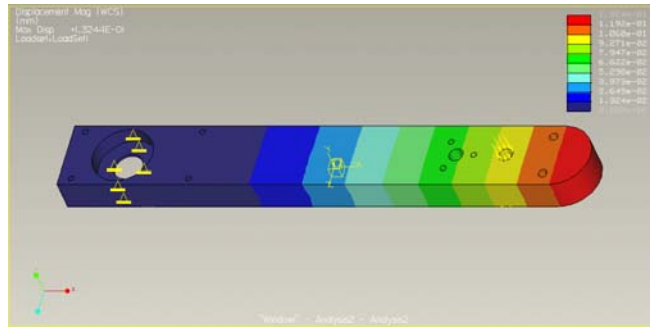


Figure 9 Displacement analysis for Link2

The safety factor calculated is 6.32. Since the safety factor is above the range of 3~5, the thickness of the Link2 is too big, resulting in material wastage. However, after considering the design of the arm joint and fabrication process of the SCARA robot, the thickness value for the Link2 is maintained at 23 mm.

6.0 DYNAMICS & MOTOR SELECTION

Since pick and place operation requires accurate positioning, the selected motor must possess certain attributes that are capable to fulfill the requirements. The motor must be able to hold its load steadily and also able to rotate to a specific angle precisely with a high repeatability. Among many motors that are available in the market, stepper motors fulfill all these requirements and was selected to actuate the SCARA robot. After the type of motor is determined, it is necessary to calculate the required torque for the motor selection. Selecting a motor may result in slow movement of the robot and may result in the motor not even moving. In order to select a proper stepper motor, the joint torque of each joint is first calculated using Lagrange-Euler formulation.

Lagrangian requires kinetic and potential energies of the manipulator. Since potential energy is zero for SCARA robot, determining the kinetic energy of the links will be sufficient. Based on Figure 5, kinetic energy of a link can be expressed as:

$$K = \frac{1}{2}mv^2 + \frac{1}{2}I\omega^2 \quad (21)$$

where v is linear velocity, ω is angular velocity, m is the point mass at the center of mass and I is the moment of inertia of the rigid body at its center of mass. For Link 1, the kinematic energy can be expressed as:

$$\begin{aligned}
K_1 &= \frac{1}{2} m_1 \left(\frac{1}{2} a_1 \dot{\theta}_1 \right)^2 + \frac{1}{2} \left(\frac{1}{12} m_1 a_1^2 \right) \omega_1^2 \\
&= \frac{1}{8} m_1 a_1^2 \dot{\theta}_1^2 + \frac{1}{24} m_1 a_1^2 \dot{\theta}_1^2 \\
&= \frac{1}{6} m_1 a_1^2 \dot{\theta}_1^2
\end{aligned} \tag{22}$$

For Link 2, based on Figure 5 and Equations (7) and (8), the Cartesian position coordinates (P_{x2}, P_{y2}) of the center of mass of the link are:

$$P_{x2} = a_1 c \theta_1 + \frac{1}{2} a_2 c \theta_{12} \tag{23}$$

$$P_{y2} = a_1 s \theta_1 + \frac{1}{2} a_2 s \theta_{12} \tag{24}$$

Differentiating Equations (23) and (24),

$$\dot{P}_{x2} = -a_1 s \theta_1 \dot{\theta}_1 - \frac{1}{2} a_2 s \theta_{12} \dot{\theta}_{12} \tag{25}$$

$$\dot{P}_{y2} = -a_1 c \theta_1 \dot{\theta}_1 + \frac{1}{2} a_2 c \theta_{12} \dot{\theta}_{12} \tag{26}$$

From these, the square of magnitude of v_2 for Link 2 is

$$\begin{aligned}
v_2^2 &= \dot{P}_{x2}^2 + \dot{P}_{y2}^2 \\
&= a_1^2 s \theta_1^2 \dot{\theta}_1^2 + \frac{1}{4} a_2^2 s \theta_{12}^2 \dot{\theta}_{12}^2 + a_1 a_2 s \theta_1 s \theta_{12} (\dot{\theta}_1^2 + \dot{\theta}_{12}^2) + a_1^2 c \theta_1^2 \dot{\theta}_1^2 \\
&\quad + \frac{1}{4} a_2^2 c \theta_{12}^2 \dot{\theta}_{12}^2 + a_1 a_2 c \theta_1 c \theta_{12} (\dot{\theta}_1^2 + \dot{\theta}_{12}^2) \\
&= a_1^2 \dot{\theta}_1^2 + \frac{1}{4} a_2^2 \dot{\theta}_{12}^2 + a_1 a_2 c \theta_2 s \theta_{12} (\dot{\theta}_1^2 + \dot{\theta}_{12}^2)
\end{aligned} \tag{27}$$

Thus, kinetic energy for Link 2 is

$$K_2 = \frac{1}{2} m_2 \left[a_1^2 \dot{\theta}_1^2 + \frac{1}{4} a_2^2 \dot{\theta}_{12}^2 + a_1 a_2 c \theta_2 (\dot{\theta}_1^2 + \dot{\theta}_{12}^2) \right] + \frac{1}{24} m_2 a_2^2 \dot{\theta}_{12}^2$$

$$= \frac{1}{2} m_2 a_1^2 \dot{\theta}_1^2 + \frac{1}{6} m_2 a_2^2 (\dot{\theta}_1^2 + \dot{\theta}_2^2 + 2 \dot{\theta}_1 \dot{\theta}_2) + \frac{1}{2} m_2 a_1 a_2 c \theta_2 (\dot{\theta}_1^2 + \dot{\theta}_{12}^2) \quad (28)$$

Lagrangian for the SCARA system is defined as

$$L = K - P = K_1 + K_2 \\ = \frac{1}{2} \left(\frac{1}{3} m_1 + m_2 \right) a_1^2 \dot{\theta}_1^2 + \frac{1}{6} m_2 a_2^2 (\dot{\theta}_1^2 + \dot{\theta}_2^2 + 2 \dot{\theta}_{12}^2) + \frac{1}{2} m_2 a_1 a_2 c \theta_2 (\dot{\theta}_1^2 + \dot{\theta}_1 \dot{\theta}_2) \quad (29)$$

Lagrange-Euler formulation for torque is given by:

$$\frac{d}{dt} \left(\frac{\partial L}{\partial \omega_i} \right) - \frac{\partial L}{\partial \theta_i} = T_i \quad \text{for } i=1,2,\dots,n \quad (30)$$

For Link 1, Lagrangian in Equation (29) is differentiated wrt θ_1 and ω_1 to give:

$$\frac{\partial L}{\partial \theta_1} = 0 \quad (31)$$

$$\frac{\partial L}{\partial \omega_1} = \frac{\partial L}{\partial \dot{\theta}_1} = \left(\frac{1}{3} m_1 + m_2 \right) a_1^2 \dot{\theta}_1 + \frac{1}{3} m_2 a_2^2 \dot{\theta}_{12} + \frac{1}{3} m_2 a_1 a_2 c \theta_2 (2 \dot{\theta}_1 + \dot{\theta}_2) \quad (32)$$

Differentiating Equation (32) wrt time,

$$\frac{d}{dt} \left(\frac{\partial L}{\partial \dot{\theta}_1} \right) = \left[\left(\frac{1}{3} m_1 + m_2 \right) a_1^2 + \frac{1}{3} m_2 a_2^2 + m_2 a_1 a_2 c \theta_2 \right] \ddot{\theta}_1 \\ + m_2 \left(\frac{1}{3} a_2^2 + \frac{1}{2} a_1 a_2 c \theta_2 \right) \ddot{\theta}_2 - m_2 a_1 a_2 s \theta_2 (\dot{\theta}_1 \dot{\theta}_2) - \frac{1}{2} m_2 a_1 a_2 s \theta_2 (\dot{\theta}_2^2) \\ = T_1 \quad (33)$$

Similarly, for Link 2,

$$\frac{\partial L}{\partial \theta_2} = -\frac{1}{2} m_2 a_1 a_2 s \theta_2 (\dot{\theta}_1^2 + \dot{\theta}_1 \dot{\theta}_2) \quad (34)$$

$$\frac{\partial L}{\partial \omega_2} = \frac{\partial L}{\partial \dot{\theta}_2} = \frac{1}{3} m_2 a_2^2 \dot{\theta}_2 + \frac{1}{2} m_2 a_1 a_2 c \theta_2 (\dot{\theta}_1) \quad (35)$$

Differentiating Equation (35) wrt time,

$$\frac{d}{dt} \left(\frac{\partial L}{\partial \dot{\theta}_2} \right) = \left(\frac{1}{3} m_2 a_2^2 + \frac{1}{2} m_2 a_1 a_2 c \theta_2 \right) \ddot{\theta}_1 + \frac{1}{3} m_2 a_2^2 \ddot{\theta}_2 - \frac{1}{2} m_2 a_1 a_2 s \theta_2 (\dot{\theta}_1 \dot{\theta}_2) \quad (36)$$

Substituting Equations (34) and (36) into Equation (30),

$$T_2 = \left(\frac{1}{3} m_2 a_2^2 + \frac{1}{2} m_2 a_1 a_2 c \theta_2 \right) \ddot{\theta}_1 + \frac{1}{3} m_2 a_2^2 \ddot{\theta}_2 + \frac{1}{2} m_2 a_1 a_2 s \theta_2 (\dot{\theta}_1)^2 \quad (37)$$

Based on parameters and a safety factor of 1.4, values for $T_{1\max}$ and $T_{2\max}$ are calculated to be 10 Nm and 4 Nm respectively. Based on this calculation, appropriate second hand brushed DC motors from Faulhaber have been selected.

7.0 ELECTRONICS

Since one of the objectives is to produce low cost robot, a simple controller using PIC16F876 microcontroller is developed. Printed circuit board (PCB) is designed using DipTrace. Figure 10 shows the schematic diagram of the controller circuit. The motor driver selected is an FD04A DC motor driver (Cytron Technologies) and has 4 channels which, suitable for the developed 4-DOF SCARA robot.

Since the DC motor used is not equipped with encoders, absolute mechanical encoders EAW0J-B24-AE0128L (Bourns) are used as encoders. The encoder has a resolution of 128 pulse per-revolution. The encoder is attached to the shaft of the motor through two identical spur gears (Figure 11).

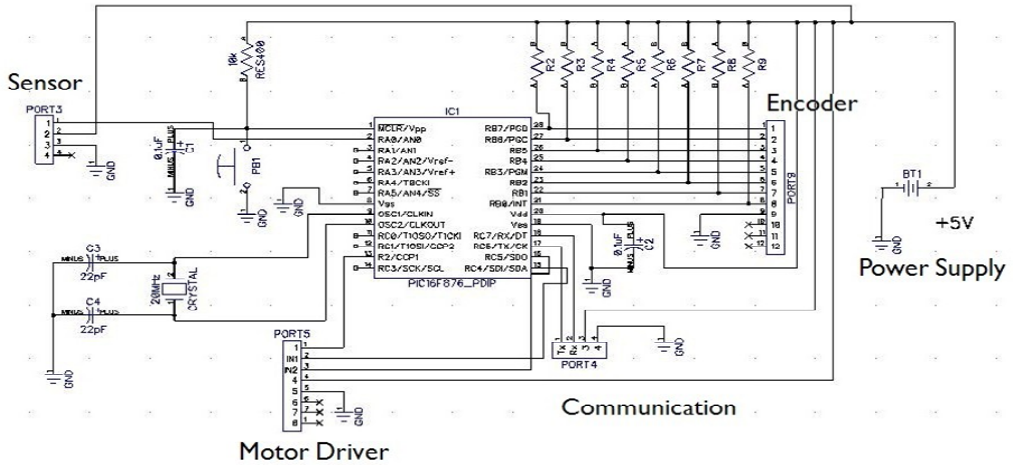


Figure 10 Schematic diagram of developed controller circuit

To avoid the linkages from colliding with each other and damaging vital components of the robot, infrared (IR) sensors are used to give feedback to the controller unit if the linkages are too close to each other. IR01A (Cytron Technologies) has the sensitivity between 2 cm to 10 cm and is compact enough to be used for the SCARA robot. Figure 12 shows the controller board connected to the respective devices including the communications port

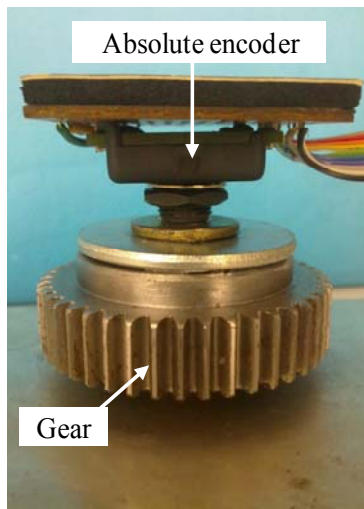


Figure 11: Mechanical absolute encoder attached to gear

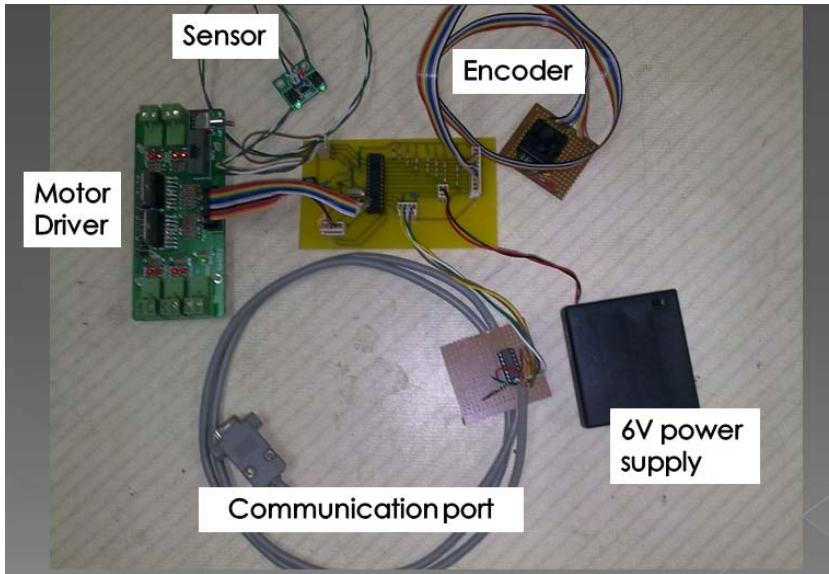


Figure 12 Controller unit connected to respective units

8.0 FABRICATION & TESTING

After carefully selecting the parts and components required, the SCARA robot is then fabricated. Figure 13 shows the completely fabricated and assembled robot. The SCARA robot's arm length for Link1 is $a_1 = 250$ mm and Link2 is $a_2 = 270$ mm. The total weight of the SCARA robot is 9.85kg. Based on experiments, the motion range for Link1 is $\pm 92.6^\circ$ and Link2 are $\pm 158^\circ$ and $\pm 150^\circ$. The execution time of the SCARA robot to reach desired position was estimated to be 2s. The 2D-working envelope of the SCARA robot was formed based on the motion range and can be seen in the Figure 14. The SCARA robot's work envelope was limited to avoid any physical contact between the end effector and other parts of the SCARA robot. The limited areas were set to be 106 mm radius from the centre of the base to avoid contacting with the base of the SCARA robot while $\pm 169^\circ$ at the centre of the base to avoid contacting with the wiring. After the limited areas were set, the work envelope of the SCARA robot was determined based on this specified area.



Figure 13 Overview of the 4-DOF SCARA robot

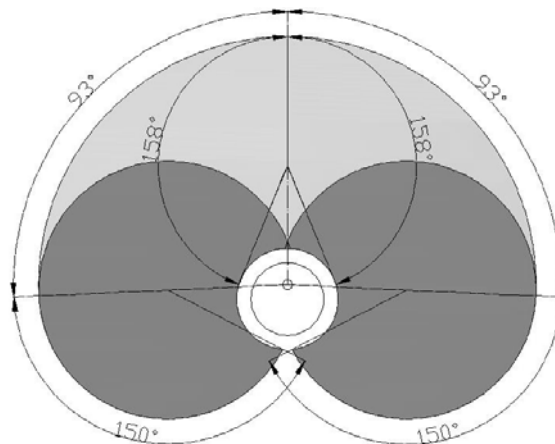


Figure 14 Working envelope of the 4-DOF SCARA robot

8.1 Basic Position & Velocity Tests

Using the algorithm designed for the robot, the robot can accurately determine whether to rotate clockwise or counter-clockwise in order to reach the desired position from current position. When it reached the desired position, the motor will stop. If the linkage over rotated due to inertia force, adjustment will be made automatically by rotating back a little bit until it reached the expected position.

When sensor detects any nearby object, input will be sent to the controller board and override every command. All motor will stop rotating to prevent linkages from clashing. Velocity tests have also been conducted and the motors run at different speeds on scale of 0 to 255.

8.2 Accuracy Test

Figure 15 shows the positions of the first linkage within the working envelope of SCARA robot arm for the accuracy test during position control. Testing is done for the first linkage since it has to support the total weight and is the most difficult to control in terms of accuracy. The idea here is to divide the position to 0° , 5° , 10° , 15° , 20° , 25° and 30° in angle. Rotation speed is fixed at 33% of the maximum speed. Table 4 shows some of the results of the test. Figure 16 shows scenes during the test.

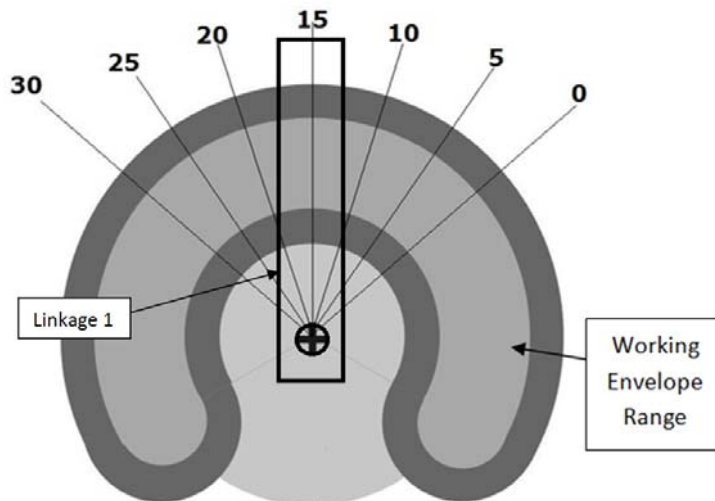


Figure 15 Positioning of Linkage 1 during accuracy test

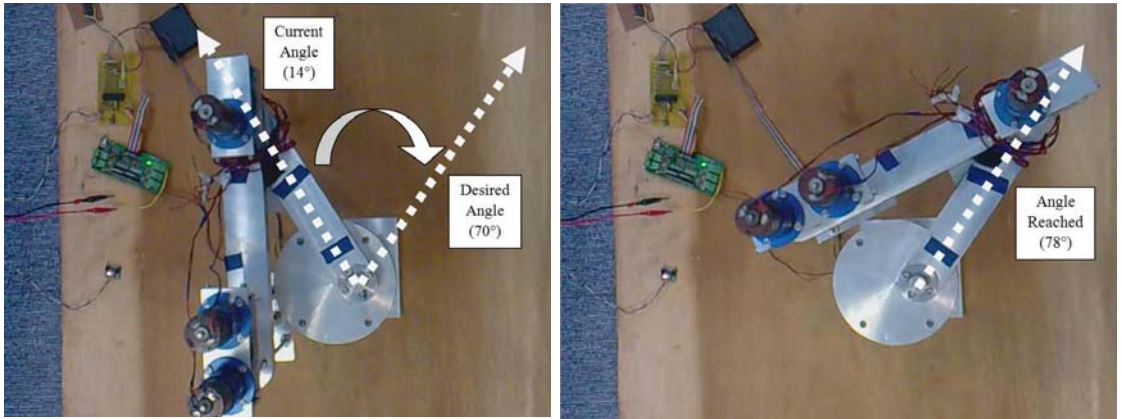


Figure 16 Scenes at the start and end of accuracy test during position control

Table 4 Results of accuracy test during position control

Current Angle (degree°)	Desired Angle (degree°)	Actual angle (degree°)	Deviation (± degree°)
14	70	78	8
78	28	18	10
34	62	69	7
6	84	92	8

From Table 4, four experiments were carried out with specific desired position and current position. Using a protractor, the deviation from the actual angle was estimated. The error is due to the weight of the linkages (inertia force acts even when the motor stops) and delay on the controller board. Overall, the error is relatively consistent except for the second experiment. Changing the controller to a faster one should solve this problem. Using bigger actuators should also give better performance and accuracy.

Payload tests were also conducted and the SCARA robot was able to carry up to 1kg of payload without fail.

9.0 CONCLUSION

A low cost 4-DOF R-R-P-R SCARA robot has been designed, developed and tested. Stress analyses and kinematics analyses have been conducted before the final prototype was developed. Dedicated controller unit is also developed for the robot. The developed prototype has also been tested to determine the working envelope and also to test its effectiveness in terms of its speed, position accuracy and maximum payload. Usage of a better microcontroller will be important to further improve the precision and processing speed. Overall, the objectives of the project have been successfully achieved. Since the robot is developed for educational purposes, other elements such as graphical user interface (GUI) ([11], [12]) and Artificial Intelligence (AI) ([12]) should also be incorporated into the robot in the near future.

ACKNOWLEDGEMENTS

The authors would like to thank Universiti Tenaga Nasional for providing research fund and equipment essential for this study.

REFERENCES

- [1] Westerlund, L. 2000. *The Extended Arm of Man: A History of the Industrial Robot*. Stockholm: Informationsförlaget.
- [2] Bhatia, P., J. Thirunarayanan, and N. Dave. 1998. An Expert System-based Design of SCARA Robot. *Expert Systems with Applications*. 15: 99-109.
- [3] Manjunath, T.C., and C. Ardil. 2007. Development of A Jacobean Model for A 4-Axes Indigenously Developed SCARA System. *Int. Journal of Computer and Information Science and Engineering*. 1(3): 152-158.
- [4] Omari, A., A. Ming, G. Liman, C. Kanamori, M. Kajitani, and S. Nakamura. 2000. Development of a High Precision Mounting Robot System with Fine Motion Mechanism (3rd Report) : Positioning Experiments of SCARA Robot with Fine Mechanism. *Journal of the Japan Society of Precision Engineerin*. 67(7):1101-1107.
- [5] Ali, H.S., L. Boutat-Baddas, Y. Becis-Aubry, and M. Darouach. 2006. H₂ Control of a Scara Robot Using Polytopic Lpv Approach. *Proceedings of the 14th Mediterranean Conference on Control and Automation*. 1-5.
- [6] Teh, S. H., S. R. Malawaraarachci, W. P. Chan, and A. Nassirharand. 2010. A Benchmark Laboratory for Experimenting with Multivariable Nonlinear Control Methodologies. *International Journal of Systems Contro*. 1(2): 62-69.
- [7] Das, M.T., and L.C. Dülger. 2005. Mathematical Modelling, Simulation and Experimental Verification of a Scara Robot. *Simulation Modelling Practice and Theory*.13(3): 257-271.
- [8] Ge, S.S., T.H. Lee, J.Q. Gong. 1999. A Robust Distributed Controller of a Single-Link SCARA/Cartezian Smart Materials Robot. *Mechatronics*. 9(1): 65-93.
- [9] Omodei, A., G. Legnani, R. Adamini. 2000. Three Methodologies for the Calibration of Industrial Manipulators: Experimental Results on A SCARA Robot. *Journal of Robotic System.s* 17(6): 291-307.

- [10] Tsai, L.W. 1999. *Robot Analysis: The Mechanics of Serial and Parallel Manipulator*. New York: John Wiley & Sons.
- [11] Hong, K.S., K.H. Choi, J.G. Kim, and S. Lee. 2001. A PC-based Open Robot Control System: PC-ORC. *Robotics and Computer Integrated Manufacturing*. 17(4): 355-365.
- [12] Er, M.J., M.T. Lim, and H.S. Lim. 2001. Real Time Hybrid Adaptive Fuzzy Control of a SCARA Robot. *Microprocessors and Microsystems*. 25(8): 369-378.